NANO LETTERS

pubs.acs.org/NanoLett Letter

Graphene Buffer Layer on SiC as a Release Layer for High-Quality Freestanding Semiconductor Membranes

Kuan Qiao,[¶] Yunpeng Liu,[¶] Chansoo Kim, Richard J. Molnar, Tom Osadchy, Wenhao Li, Xuechun Sun, Huashan Li, Rachael L. Myers-Ward, Doyoon Lee, Shruti Subramanian, Hyunseok Kim, Kuangye Lu, Joshua A. Robinson, Wei Kong,* and Jeehwan Kim*

Cite This: *Nano Lett.* 2021, 21, 4013−4020 Read Online

ACCESS | Metrics & More | Article Recommendations | Supporting Information

ABSTRACT: Free-standing crystalline membranes are highly desirable owing to recent developments in heterogeneous integration of dissimilar materials. Van der Waals (vdW) epitaxy enables the release of crystalline membranes from their substrates. However, suppressed nucleation density due to low surface energy has been a challenge for crystallization; reactive materials synthesis environments can induce detrimental damage to vdW surfaces, often leading to failures in membrane release. This work demonstrates a novel platform based on graphitized SiC for fabricating high-quality free-standing membranes. After mechanically removing epitaxial graphene on a graphitized SiC wafer, the quasi-two-dimensional graphene buffer layer (GBL) surface remains intact for epitaxial growth. The reduced vdW gap between the epilayer and substrate enhances epitaxial interaction, promoting remote epitaxy. Significantly improved nucleation and convergent quality of GaN are achieved on the GBL, resulting in the best quality GaN ever grown on two-dimensional materials. The GBL surface exhibits excellent resistance to harsh growth environments, enabling substrate reuse by repeated growth and exfoliation.

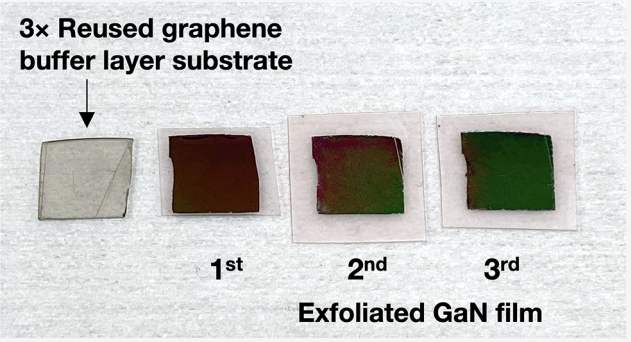

KEYWORDS: *GaN, SiC, ZnO, graphitization, buffer layer*

The free-standing membranes of wide-bandgap semiconductors can provide extra degrees of freedom in their functional implementations, while the planar form factor is compatible with modern electronic processing allowing production scalability. For example, on-chip strain and acceleration sensing is achieved by using a free-standing GaN-based transistor, with which device output can be modulated by deformation.[1] Without the substrate's restraint, high magnetostriction and piezoelectricity are achieved by the heterointegration of free-standing complex oxide membranes.[2] Additionally, the adoption of free-standing membranes instead of bulk materials provides significant cost savings to produce electronics, of which the major cost is usually material related. Producing free-standing crystalline thin-film semiconductors requires the separation of epitaxial crystalline thin films from their substrates. Previously, van der Waals epitaxy emerged as a solution, as the weak van der Waals interface provides a mechanism for the release of crystalline membranes.[3,4] However, it is challenging for van der Waals epitaxy to realize high-quality crystallization on two-dimensional (2D) materials while having releasable epitaxial films, especially in the case of non-polar 2D material such as graphene. During van der Waals epitaxy, nucleation density and crystalline alignment on the van der Waals surface are significantly suppressed due to the low surface free energy, leading to poor convergence or even failure in film formation. For example, directly growing GaAs or GaN on graphene tends to produce micro- and nanorods.[5−7] The orientation of GaAs or GaN unit cells is observed not strictly aligned to that of graphene unit cells during the van der Waals epitaxy process due to the weak interactions.[8,9] In the reports that show GaN layer exfoliation, rough surface morphology and polycrystalline structure are often observed.[10−12] Moreover, 2D materials are susceptible to damage due to the harsh ambient where crystalline semiconductor thin films are produced. Damaged 2D materials and the associated defective van der Waals surfaces can lead to failure in releasing the membranes. For example, the graphene used for GaN growth can be damaged by H_2 carrier gas during growth at high growth temperature[13] and by NH_3 or nitrogen plasma during metal organic chemical vapor deposition (MOCVD) or

Received: February 24, 2021
Revised: April 20, 2021
Published: April 26, 2021

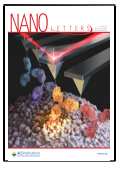

https://doi.org/10.1021/acs.nanolett.1c00673
Nano Lett. 2021, 21, 4013−4020

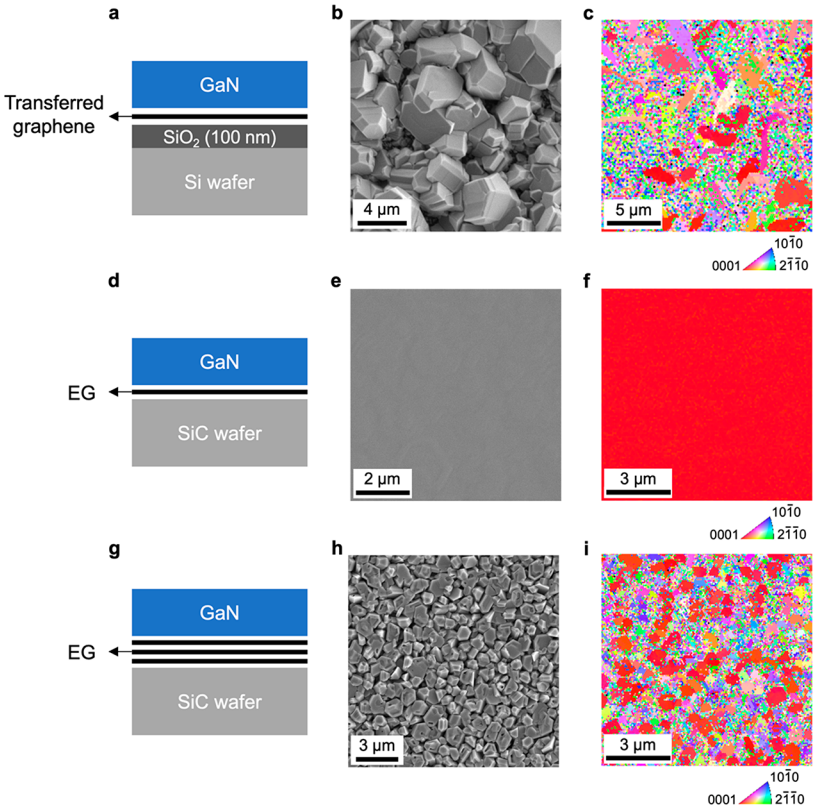

Figure 1. Seeding capability of graphene. Schematic (a), scanning electron microscopy (SEM) image (b) and electron backscatter diffraction (EBSD) map (c) of GaN grown on graphene transferred on SiO_2/Si. Schematic (d), SEM image (e), and EBSD map (f) of GaN grown on graphitized SiC substrate with monolayer EG. Schematic (g), SEM image (h), and EBSD map (i) of GaN grown on graphitized SiC substrate with three layers of EG.

molecular beam epitaxy (MBE) growth.[14,15] Simultaneously achieving a high-quality epilayer and maintaining a robust van der Waals surface, which is the key to fabricating free-standing single-crystalline semiconductor membranes, has been one of the greatest challenges faced by the community.

In this study, we reveal a new mechanism of having high-quality single-crystalline membranes on a 2D interface while allowing a high yield release of membranes without damaging the wafer to ensure reusability of the substrate. First of all, to achieve high-quality crystalline thin films on 2D materials, an enhanced seeding effect from the substrate is desirable. Meanwhile, to ensure the substrate is reusable without damaging the van der Waals surface, strong adhesion of the 2D material to the substrate is needed in harsh material growth environments. We discovered that these conditions can be simultaneously satisfied by a modification of a graphitized SiC(0001) wafer which consists of epitaxial graphene (EG) on top of an interfacial graphene buffer layer (GBL) on the SiC wafer.[16] The GBL contains a graphene-like honeycomb lattice with lateral sp^2-bonded carbon atoms, while it bonds to the SiC substrate by sp^3-hybridized covalent bonds.[17−21] Meanwhile, the GBL is fully covered by EG, which is connected to the substrate only via van der Waals force. Our previous study experimentally determined that the adhesion energy between EG and the SiC substrate is 106 meV/atom.[22] Although no exact value of the bond energy between the GBL and SiC substrate has been reported, it should fall within the range of 2−5 eV/atom, which is the typical energy for a covalent bond. This stark contrast in bonding strength enables us to mechanically remove the EG from the wafer, allowing the exposure of the GBL. Strong adhesion of the GBL to the substrate leads to resistance to harsh growth conditions of GaN or ZnO, while the quasi-2D surface permits the release of the epilayer. The GBL can endure multiple growth−release cycles to ensure the release of epitaxial films with 100% yield from the SiC substrate with possible substrate reuse. Meanwhile, the proximity of the GBL to SiC substrate enhances the potential field transmitted through the GBL so that remote epitaxy can be facilitated, since the strength of the remote interaction is inversely proportional to the distance between the substrate and the epilayer.[23,24] Through this process, we successfully demonstrated releasable GaN epitaxial films on a GBL substrate with the best crystalline quality ever reported for releasable GaN thin film, with a dislocation density of 2.1×10^7 cm^{-2}. We further proved that the quasi-2D surface of the GBL can endure O_2 plasma introduced during ZnO growth, in which case either EG or transferred graphene would be etched away completely.

RESULTS AND DISCUSSION

While van der Waals epitaxy of GaN on graphene has been extensively studied, high-quality single-crystalline growth and exfoliation of GaN on graphene has not been widely reported. This is a result of the weak interaction and non-polar nature of C−C bonding in graphene.[24] First, we investigated the feasibility of graphene as a seeding layer for GaN epitaxy. A monolayer single-crystalline EG was exfoliated from a graphitized SiC and transferred on a Si thermal oxide wafer, which has an amorphous SiO_2 layer on top. To prevent nucleation at defect sites, the EG had not undergone any

https://doi.org/10.1021/acs.nanolett.1c00673
Nano Lett. 2021, 21, 4013−4020

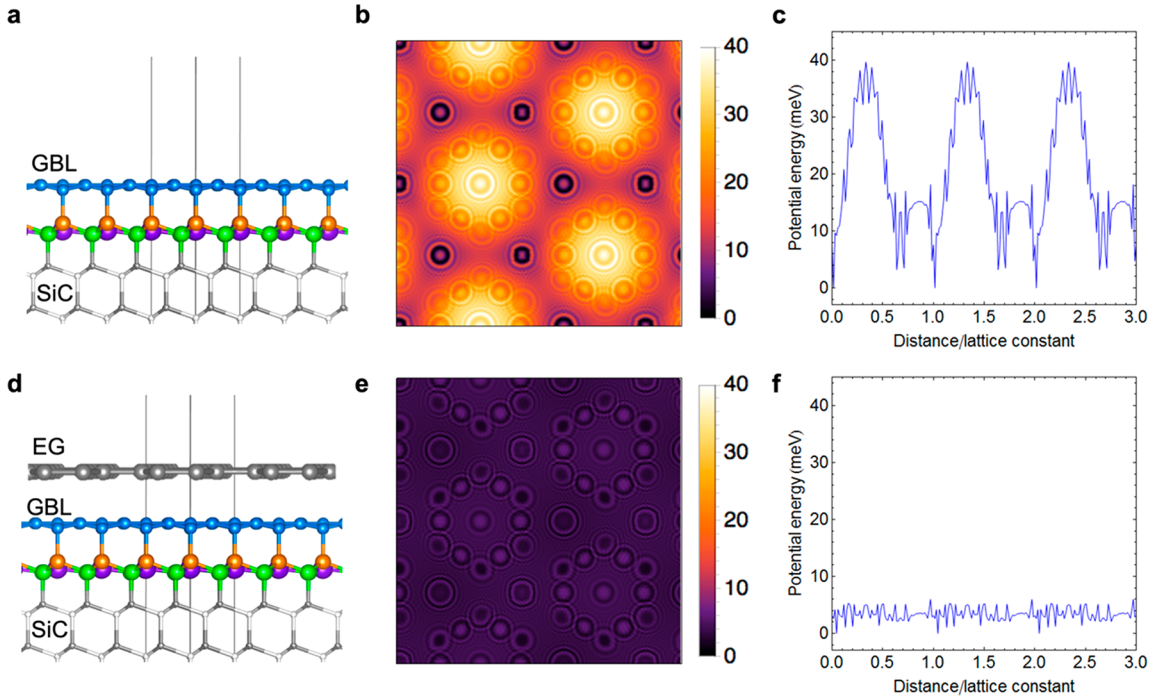

Figure 2. Density functional theory (DFT) calculation for field penetration. (a) Modeled atomic structures of the buffer layer on SiC, (b) potential fluctuation (meV) maps on the GBL, and (c) potential fluctuations across the horizontal direction on the GBL. (d) Modeled atomic structures of as-graphitized SiC. (e) Potential fluctuation (meV) maps on EG. (f) Potential fluctuations across the horizontal direction on EG.

intentional damaging processes.[25−27] Given the amorphous nature of the SiO_2 substrate, the crystalline orientation can only be seeded from the transferred EG. Subsequently, we deposited GaN on the transferred graphene surface. The structure of the sample is illustrated in Figure 1a. As shown in the scanning electron microscopy (SEM) image of the as-grown surface (Figure 1b) and the electron backscatter diffraction (EBSD) mapping (Figure 1c), we confirmed that the GaN grown on EG/SiO_2 is polycrystalline. This result indicates that EG fails to induce epitaxial orientation at the initial stage of growth due to its weak surface interactions. As a comparison, we also deposited GaN directly on a monolayer EG surface, where a crystalline SiC substrate is beneath the monolayer graphene (structure shown in Figure 1d). As shown in Figure 1e and f, the GaN grown on the EG/SiC substrate exhibits well-aligned crystalline planes. The contrasting results from this set of experiments suggest that the orientation of the GaN epilayer originates from the underlying substrate, rather than the EG. As further confirmation, we deposited GaN on three monolayers (3 ML) of EG as-grown on SiC (structure shown in Figure 1g). In this case, the GaN epilayer and SiC substrate are decoupled by the gap consisting of three to four layers of EG. As parts h and i of Figure 1 show, the deposited GaN showed polycrystalline formation, confirming the fact that pristine graphene is not the source of epitaxial seeding to GaN, but the potential field transmitted through graphene from the substrate is responsible for single-crystalline GaN growth on EG substrate.[24] The results also suggest that single-crystalline GaN grown on EG previously reported is likely caused by remote epitaxial seeding from the substrate rather than van der Waals epitaxial seeding from the graphene.[28]

Although the field from the SiC can induce orientation alignment across monolayer EG to form epitaxial GaN, the epitaxial interaction attenuates with an increasing distance. The reduced epitaxial interaction in turn can weaken the seeding effects, in terms of nucleation density and quality, thus forming a high density of crystalline defects.[24] Excessive defects severely degrade the performance of electronic devices. Here we developed a method to substantially enhance the epitaxial interactions between the epilayer and the substrate to obtain high-quality GaN epitaxial films on graphitized SiC. It is well-known that the growth of monolayer EG on SiC is mediated by the formation of an interfacial GBL on SiC substrates upon graphitization and the GBL also has graphene-like hexagonal lattices, maintaining its in-plane sp^2 bonding properties on the surface while it strongly adheres to the substrate via sp^3 bonds. Thus, if the GBL can be exposed to directly interact with adatoms during growth without having an EG layer, the epilayer−substrate distance could be substantially reduced. Thus, it will enhance the epitaxial interaction and crystallization quality, while the epitaxial layers may still be released from the sp^2 bonded GBL surface. We theoretically investigated the hypothesis by DFT calculations of the potential distribution from the SiC substrate penetrating through the GBL. The atomic structures of SiC surfaces without and with EG are illustrated in Figure 2a and d, respectively. Compared with the van der Waals interaction between EG and the GBL, the GBL is connected with the SiC substrate via Si−C covalent bonding, which suggests the robustness of the GBL in harsh environments. Given the desired lattice matching between SiC crystal and EG, slight distortion is observed in the GBL with its planar structure almost preserved. Figure 2b and e show maps of potential fluctuation (the difference between potential energy maxima and minima along the surface of the substrate) contributed by the substrate (SiC and GBL) at a distance to the epitaxial GaN layer (3.5 Å) on both the GBL and as-graphitized SiC. The calculation indicates that the atomic interaction between the epilayer and the SiC substrate is well maintained at the GBL surface by preserving the strong potential fluctuation from the

https://doi.org/10.1021/acs.nanolett.1c00673
Nano Lett. 2021, 21, 4013−4020

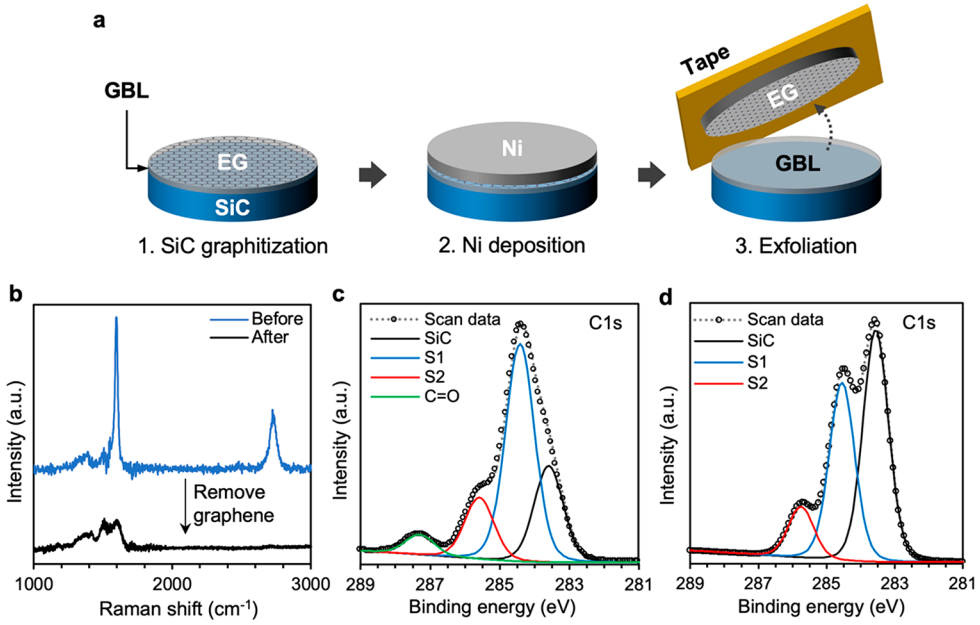

Figure 3. GBL substrate fabrication. (a) Schematic of the process of EG exfoliation. (b) Raman spectrum of graphitized SiC before (blue) and after (black) removing the EG. (c) X-ray photoelectron spectroscopy (XPS) C 1s spectra of EG. (d) X-ray photoelectron spectroscopy (XPS) C 1s spectra of the GBL after the EG is removed.

substrate (Figure 2c). In contrast, the epilayer−substrate interaction at the EG surface is substantially reduced (Figure 2f), as a result of the drastic decay of potential fluctuation with increasing distance.

The above DFT calculation supports our experimental investigation of utilizing the surface of the GBL instead of EG, in order to strengthen the interactions between the epitaxial layer and the SiC substrate. Achieving a full coverage GBL on SiC is challenging, because the conventional graphitization process tends to self-terminate with complete EG coverage. We obtain the GBL through a different approach by mechanically removing the EG from a graphitized SiC surface with a metal-induced 2D material transfer process (Figure 3a).[22] The EG was exfoliated by a layer of tensile-stressed Ni. Because the adhesion of Ni to EG is greater than that of EG to the substrate, the EG can be repeatedly exfoliated by the Ni stressor with a yield of over 95%.[22] As shown in Figure 3b, the Raman spectrum of the substrate shows the absence of the EG after peeling, but the GBL remains on the surface, as evidenced by the C 1s core level X-ray photoelectron spectroscopy (XPS) spectrum (see Figure 3c,d). The peak labeled SiC is attributed to the Si−C bonds in the SiC substrate. The components S1 and S2 respectively correspond to sp^2 and sp^3 hybridized C atoms within the GBL and EG layers. The XPS spectra of the substrate after EG removal (Figure 3d) show a significantly reduced S1 component and a consistent S2 component, indicating that the GBL still remains. The selective removal of EG is explained by the weaker adhesion of EG to the substrate by van der Waals force than that of the GBL by covalent bonding to the substrate.

After removing the EG, we deposited GaN on the GBL and observed the nucleation process. We found that nucleation density was substantially enhanced on the GBL/SiC substrate compared to that on the EG/GBL/SiC substrate, as shown in Figure 4a and b. The subsequential growth of 5 μm of GaN on GBL/SiC shows improved crystalline quality compared to that on EG/GBL/SiC. The atomic force microscopy (AFM) image in Figure 4c shows a smooth as-grown surface of the GaN grown on GBL/SiC with a root-mean-square (RMS) roughness of 0.18 nm. The triple-axis high-resolution X-ray diffraction (HRXRD) ω-scan of GaN(002) and (105) peaks for the GaN epilayer on the GBL are reduced from 328 to 141 arcsec and from 279 to 193 arcsec in comparison to those of GaN grown on EG/GBL/SiC, as shown in Figure 4e and f. The corresponding screw dislocation density and edge dislocation density estimated from the fwhm are reduced from 2×10^8 to 4×10^7 cm^{-2} and from 5×10^8 to 2×10^8 cm^{-2}, respectively.[29] The HRXRD ϕ-scan in Figure 4g confirms a well-aligned in-plane 6-fold symmetry. In Figure 4d, the electron channeling contrast imaging (ECCI) image of the GaN grown on the GBL shows a total threading dislocation density of 2.1×10^7 cm^{-2}, correlating well with the HRXRD analysis. To the best of our knowledge, the GaN grown on the GBL demonstrated in this work has the lowest dislocation density reported for GaN directly grown on 2D materials or other van der Waals surfaces.

Although the GBL is covalently bonded to SiC, the graphene-like quasi-2D surface still provides the van der Waals surface for the release of epilayers from the substrate. We demonstrated the complete release of GaN membranes from the surface of the GBL, as shown in Figure 4h. After releasing GaN, the XPS spectra of the substrate confirmed that the GBL remained on the surface (Figure 4i), while the surface of the substrate remains undamaged with a smooth morphology, as shown by the AFM image in Figure 4j. This makes a clear contrast to the case where the GaN was grown on graphene transferred onto a host substrate, which has been the prevalent approach for previous studies on GaN-on-graphene. Although we adopted the same growth conditions for GaN on the GBL, GaN grown on transferred graphene by MOCVD was not exfoliated for repeated trials. This could be attributed to the poor resistance of transferred graphene to harsh MOCVD growth conditions which typically involves a corrosive ambient with NH_3 and H_2 at high temperature.[13] To

https://doi.org/10.1021/acs.nanolett.1c00673
Nano Lett. 2021, 21, 4013−4020

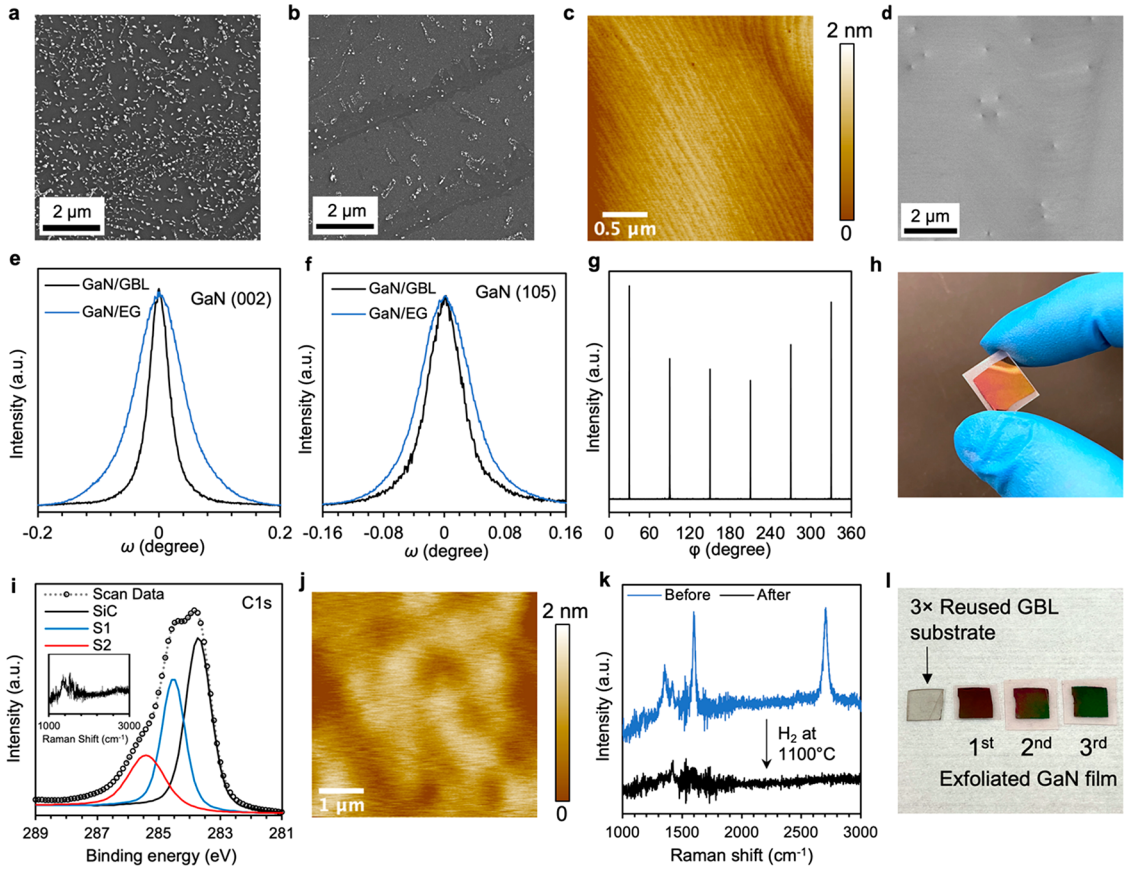

Figure 4. GaN growth on EG and the GBL. (a) SEM image of GaN nucleation grown on EG. (b) SEM image of GaN grown on the GBL. (c) Atomic force microscopy (AFM) image of the surface of the GaN grown on the GBL. The RMS roughness is 0.18 nm. (d) Electron channeling contrast imaging (ECCI) image of GaN grown on the GBL, showing a total threading dislocation density of 2.1×10^7 cm^{-2}. (e) High-resolution X-ray diffraction (HRXRD) rocking curves of GaN(002) on the GBL and EG. (f) HRXRD rocking curves of GaN(105) on the GBL and EG. (g) HRXRD ϕ-scan of GaN grown on the GBL. (h) Photograph of exfoliated GaN on the GBL thin film on a flexible substrate (thermal release tape). (i) C 1s XPS spectrum of the GBL substrate after GaN epilayer exfoliation, and the inset shows its Raman spectrum. (j) AFM image of the GBL substrate after GaN epilayer exfoliation. (k) Raman spectra of transferred graphene on SiC before and after treating in H_2 at 1100 °C. (l) Photograph of the three-times-reused GBL substrate and the exfoliated GaN epilayers.

better understand the damaging process of graphene, we simulated the MOCVD growth environment with an annealing test at 1100 °C in H_2 ambient; we found that transferred graphene was completely etched away after 10 min (see the Raman results before and after H_2 treatment in Figure 4k). These findings indicate that the covalent adhesion of the GBL to the substrate prevents the etching of sp^2-bonded carbon on the surface in the harsh MOCVD growth environment, resulting in repeatable exfoliation.[22] While MOCVD conditions could damage transferred graphene, such damage can be mitigated by performing the growth using MBE. As shown in Figure S1, MBE-grown GaN was successfully exfoliated from transferred graphene because H_2 gas is not involved and the substrate temperature is much lower in MBE growth. However, it is difficult to avoid the formation of defects and holes in graphene during the manual graphene transfer process. Thus, the GaN growth through the defects and holes forms direct contacts with the substrate, resulting in spalling marks through the holes/defects of the graphene during exfoliation, causing severe damage of the substrate (Figure S1c,d). The situation was much improved for the case of the GBL, as shown by the XPS spectrum in Figure 4i, where the surface of the substrate after epilayer exfoliation is still well covered with the GBL, indicated by the unchanged S2 component. In Figure 4j, the AFM image of the reused substrate shows an undamaged surface due to the full coverage of the robust GBL on SiC. This enables us to reuse the same substrate three times without re-graphitizing or any polishing process. Only a standard wafer cleaning process is required between two GaN growths (see the Supporting Information). The photographs of the three-times-reused substrate and the exfoliated epilayers are shown in Figure 4l.

In addition, we proved that the GBL can even endure highly reactive O_2 plasma environments, in which case typical graphene, even EG, would be immediately damaged or removed completely. As shown in Figure 5b, the C 1s XPS spectra of the GBL after a 10 min O_2 plasma treatment show an unchanged S2 component compared with the one before the treatment (Figure 5a), indicating the sp^3 bonds between the GBL and SiC are unchanged and thus an undamaged GBL/SiC interface. In contrast, the Raman spectrum of the EG before and after the same O_2 plasma treatment shown in Figure 5c indicates that the EG was etched during the O_2 plasma treatment. As a demonstration, we performed remote epitaxy of ZnO on the GBL substrate by using magnetron sputtering with O_2 plasma. Figure 5d shows the AFM image of the surface of the as-grown ZnO on the GBL. The HRXRD $2\theta-\omega$ and the ϕ-scan of as-grown ZnO on the GBL indicate

https://doi.org/10.1021/acs.nanolett.1c00673
Nano Lett. 2021, 21, 4013−4020

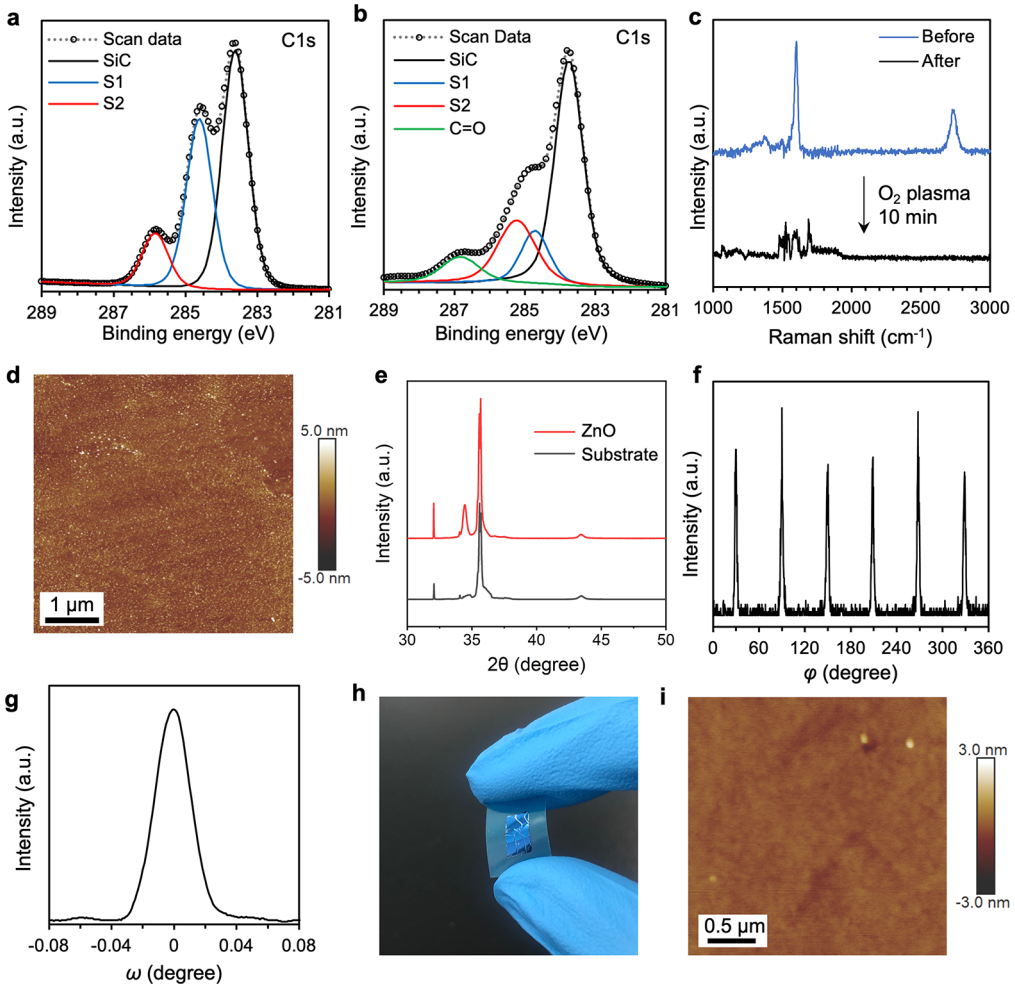

Figure 5. ZnO growth on the GBL. XPS C 1s spectrum of the GBL before (a) and after (b) a 10 min O_2 plasma treatment. (c) Raman spectra of EG on SiC before and after a 10 min O_2 plasma treatment. (d) AFM scan of the surface of as-grown ZnO deposited on the GBL substrate. (e) XRD 2θ-ω-scan of epitaxial ZnO showing single out-of-plane alignment. (f) XRD ϕ-scan epitaxial ZnO showing single in-plane alignment. (g) ω-Scan rocking curve of epitaxial ZnO showing a fwhm of 105 arcsec. (h) Photograph of the released ZnO film on a flexible substrate (thermal release tape). (i) AFM image of the released surface of the GBL substrate, with a 0.4 nm RMS roughness.

the 6-fold symmetric ZnO lattices free of polycrystalline phase, as shown in Figure 5e and f, confirming the single crystallinity of remote epitaxial ZnO. Furthermore, the ω-scan rocking curve (Figure 5g) shows a narrow fwhm of 105 arcsec, indicating high crystalline quality of ZnO thin film on the GBL. The undamaged GBL surface was evidenced by the complete exfoliation of the ZnO epilayer, as shown in Figure 5h. Finally, the AFM scan (see Figure 5i) of the released surface of the GBL substrate remains atomically flat. Note that, in Figure 5b, a reduced S1 component and an additional C═O peak are observed after the O_2 plasma exposure. It suggests a partial oxidation of sp^2 C−C bonds in the GBL, but this has not affected the growth and exfoliation of single-crystalline ZnO thin films, proving that the GBL could be a robust epitaxial template for a range of wide-bandgap materials, most of which require harsh synthesizing conditions.

CONCLUSIONS

In summary, we discovered that, after mechanically removing the monolayer EG on a graphitized SiC(0001) wafer, the GBL surface remains intact on the wafer, which provides a quasi-2D surface. The reduced van der Waals gap due to the removal of EG enhances the epitaxial interaction between the epilayer and the SiC substrate, promoting remote epitaxy. This method allows us to achieve 100% releasable high-quality GaN and ZnO thin films. This finding suggests that the GBL substrate could potentially be a universal platform for fabricating free-standing thin films of a wide range of materials. Due to the strong epitaxial interaction between the epilayer and substrate, the suitable materials for growing on the GBL substrate are similar to those that are suitable for heteroepitaxy on SiC—materials with hexagonal lattices and similar lattice parameters and thermal expansion coefficients to SiC are preferred. It also means that the challenges of heteroepitaxy on SiC still exist when growing materials on the GBL substrate. For example, due to the large thermal expansion coefficient mismatch between GaN and SiC, the cracking of GaN film on the GBL is observed during the post-growth cooling if GaN growth exceeds a certain thickness.[30] It remains to be further investigated if the critical cracking behavior of GaN on the GBL varies compared to that of GaN directly on SiC. Furthermore, we have proved that the GBL surface exhibits excellent resistance to the harsh growth environments involving H_2 at high temperature or O_2 plasma, enabling the consistent reuse of the substrates.

https://doi.org/10.1021/acs.nanolett.1c00673
Nano Lett. 2021, 21, 4013−4020

■ ASSOCIATED CONTENT

Supporting Information

The Supporting Information is available free of charge at https://pubs.acs.org/doi/10.1021/acs.nanolett.1c00673.

Methods and Figure S1 (PDF)

■ AUTHOR INFORMATION

Corresponding Authors

Wei Kong − *School of Engineering and Key Laboratory of 3D Micro/Nano Fabrication and Characterization of Zhejiang Province, School of Engineering, Westlake University, Hangzhou, Zhejiang 310024, China*; Email: kongwei@westlake.edu.cn

Jeehwan Kim − *Department of Mechanical Engineering, Department of Materials Science and Engineering, and Research Laboratory of Electronics, Massachusetts Institute of Technology, Cambridge, Massachusetts 02139, United States*; orcid.org/0000-0002-1547-0967; Email: jeehwan@mit.edu

Authors

Kuan Qiao − *Department of Mechanical Engineering, Massachusetts Institute of Technology, Cambridge, Massachusetts 02139, United States*

Yunpeng Liu − *Department of Mechanical Engineering, Massachusetts Institute of Technology, Cambridge, Massachusetts 02139, United States*

Chansoo Kim − *Department of Mechanical Engineering, Massachusetts Institute of Technology, Cambridge, Massachusetts 02139, United States*

Richard J. Molnar − *MIT Lincoln Laboratory, Lexington, Massachusetts 02421, United States*

Tom Osadchy − *MIT Lincoln Laboratory, Lexington, Massachusetts 02421, United States*

Wenhao Li − *School of Engineering, Westlake University, Hangzhou, Zhejiang 310024, China*

Xuechun Sun − *School of Engineering, Westlake University, Hangzhou, Zhejiang 310024, China*

Huashan Li − *School of Physics, Sun Yat-Sen University, Guangzhou, Guangdong 510275, China*

Rachael L. Myers-Ward − *U.S. Naval Research Laboratory, Washington, DC 20375, United States*

Doyoon Lee − *Department of Mechanical Engineering, Massachusetts Institute of Technology, Cambridge, Massachusetts 02139, United States*

Shruti Subramanian − *Department of Materials Science and Engineering, The Pennsylvania State University, University Park, Pennsylvania 16802, United States*; orcid.org/0000-0002-8933-9486

Hyunseok Kim − *Department of Mechanical Engineering, Massachusetts Institute of Technology, Cambridge, Massachusetts 02139, United States*

Kuangye Lu − *Department of Mechanical Engineering, Massachusetts Institute of Technology, Cambridge, Massachusetts 02139, United States*

Joshua A. Robinson − *Department of Materials Science and Engineering, The Pennsylvania State University, University Park, Pennsylvania 16802, United States*; orcid.org/0000-0002-1513-7187

Complete contact information is available at: https://pubs.acs.org/10.1021/acs.nanolett.1c00673

Author Contributions

[¶]K.Q. and Y.L. contributed equally. K.Q., Y.L., and J.K. conceived the experimental work. C.K. prepared the GBL substrates. R.J.M. and T.O. contributed to the synthesis of GaN. W.L., X.S., and W.K. contributed to the synthesis and exfoliation of ZnO. H.L. performed the DFT calculation. R.L.M.-W., S.S., and J.A.R. contributed to SiC graphitization. D.L. performed the etching test of the GBL. All of the authors contributed to the discussions and analysis of the results regarding the manuscript. J.K. directed the team.

Notes

The authors declare no competing financial interest.

■ ACKNOWLEDGMENTS

This work is supported by Future Semiconductor Business, Inc. This material is, in part, based upon work supported by the Under Secretary of Defense for Research and Engineering under Air Force Contract No. FA8702-15-D-0001. Any opinions, findings, conclusions, or recommendations expressed in this material are those of the author(s) and do not necessarily reflect the views of the Under Secretary of Defense for Research and Engineering.

■ ABBREVIATIONS

GaN, gallium nitride; SiC, silicon carbide; vdW, van der Waals; GBL, graphene buffer layer; ZnO, zinc oxide; 2D, two-dimensional; GaAs, gallium arsenide; MOCVD, metal organic chemical vapor deposition; MBE, molecular beam epitaxy; EG, epitaxial graphene; SiO_2, silicon dioxide; SEM, scanning electron microscopy; EBSD, electron backscatter diffraction; ML, monolayer; DFT, density functional theory; XPS, X-ray photoelectron spectroscopy; AFM, atomic force microscopy; RMS, root-mean-square; HRXRD, high-resolution X-ray diffraction; ECCI, electron channeling contrast imaging

■ REFERENCES

(1) Zhang, S.; Ma, B.; Zhou, X.; Hua, Q.; Gong, J.; Liu, T.; Cui, X.; Zhu, J.; Guo, W.; Jing, L.; Hu, W.; Wang, Z. L. Strain-Controlled Power Devices as Inspired by Human Reflex. *Nat. Commun.* **2020**, *11* (1), 326.

(2) Kum, H. S.; Lee, H.; Kim, S.; Lindemann, S.; Kong, W.; Qiao, K.; Chen, P.; Irwin, J.; Lee, J. H.; Xie, S.; Subramanian, S.; Shim, J.; Bae, S.-H.; Choi, C.; Ranno, L.; Seo, S.; Lee, S.; Bauer, J.; Li, H.; Lee, K.; Robinson, J. A.; Ross, C. A.; Schlom, D. G.; Rzchowski, M. S.; Eom, C.-B.; Kim, J. Heterogeneous Integration of Single-Crystalline Complex-Oxide Membranes. *Nature* **2020**, *578* (7793), 75−81.

(3) Koma, A.; Sunouchi, K.; Miyajima, T. Fabrication and Characterization of Heterostructures with Subnanometer Thickness. *Microelectron. Eng.* **1984**, *2* (1−3), 129−136.

(4) Koma, A. Van Der Waals Epitaxy—a New Epitaxial Growth Method for a Highly Lattice-Mismatched System. *Thin Solid Films* **1992**, *216* (1), 72−76.

(5) Kumaresan, V.; Largeau, L.; Madouri, A.; Glas, F.; Zhang, H.; Oehler, F.; Cavanna, A.; Babichev, A.; Travers, L.; Gogneau, N.; Tchernycheva, M.; Harmand, J.-C. Epitaxy of GaN Nanowires on Graphene. *Nano Lett.* **2016**, *16* (8), 4895−4902.

(6) Fernández-Garrido, S.; Ramsteiner, M.; Gao, G.; Galves, L. A.; Sharma, B.; Corfdir, P.; Calabrese, G.; De Souza Schiaber, Z.; Pfüller, C.; Trampert, A.; Lopes, J. M. J.; Brandt, O.; Geelhaar, L. Molecular Beam Epitaxy of GaN Nanowires on Epitaxial Graphene. *Nano Lett.* **2017**, *17* (9), 5213−5221.

(7) Mulyo, A. L.; Rajpalke, M. K.; Kuroe, H.; Vullum, P.-E.; Weman, H.; Fimland, B.-O.; Kishino, K. Vertical GaN Nanocolumns Grown on Graphene Intermediated with a Thin AlN Buffer Layer. *Nanotechnology* **2019**, *30* (4), 049601.

(8) Fuke, S.; Sasaki, T.; Takahasi, M.; Hibino, H. In-Situ X-Ray Diffraction Analysis of GaN Growth on Graphene-Covered Amorphous Substrates. *Jpn. J. Appl. Phys.* **2020**, *59* (7), 070902.
(9) Gohda, Y.; Tsuneyuki, S. Structural Phase Transition of Graphene Caused by GaN Epitaxy. *Appl. Phys. Lett.* **2012**, *100* (5), 053111.
(10) Li, T.; Liu, C.; Zhang, Z.; Yu, B.; Dong, H.; Jia, W.; Jia, Z.; Yu, C.; Gan, L.; Xu, B. GaN Epitaxial Layers Grown on Multilayer Graphene by MOCVD. *AIP Adv.* **2018**, *8* (4), 045105.
(11) Yoo, H.; Chung, K.; In Park, S.; Kim, M.; Yi, G.-C. Microstructural Defects in GaN Thin Films Grown on Chemically Vapor-Deposited Graphene Layers. *Appl. Phys. Lett.* **2013**, *102* (5), 051908.
(12) Su, J.; Liang, D.; Zhao, Y.; Yang, J.; Chang, H.; Duan, R.; Wang, J.; Sun, L.; Wei, T. Freestanding GaN Substrate Enabled by Dual-Stack Multilayer Graphene via Hydride Vapor Phase Epitaxy. *Appl. Surf. Sci.* **2020**, *526*, 146747.
(13) Park, J.; Lee, J.; Park, M.; Min, J.; Lee, J.; Yang, X.; Kang, S.; Kim, S.; Jeong, W.; Amano, H.; Lee, D. Influence of Temperature-Dependent Substrate Decomposition on Graphene for Separable GaN Growth. *Adv. Mater. Interfaces* **2019**, *6* (18), 1900821.
(14) Wang, Z.; Wei, M.; Jin, L.; Ning, Y.; Yu, L.; Fu, Q.; Bao, X. Simultaneous N-Intercalation and N-Doping of Epitaxial Graphene on 6H-SiC(0001) through Thermal Reactions with Ammonia. *Nano Res.* **2013**, *6* (6), 399−408.
(15) Yadav, R.; Dixit, C. K. Synthesis, Characterization and Prospective Applications of Nitrogen-Doped Graphene: A Short Review. *J. Sci. Adv. Mater. Devices* **2017**, *2* (2), 141−149.
(16) Trammell, S.; Hernández, S.; Myers-Ward, R.; Zabetakis, D.; Stenger, D.; Gaskill, D.; Walton, S. Plasma-Modified, Epitaxial Fabricated Graphene on SiC for the Electrochemical Detection of TNT. *Sensors* **2016**, *16* (8), 1281.
(17) Varchon, F.; Feng, R.; Hass, J.; Li, X.; Nguyen, B. N.; Naud, C.; Mallet, P.; Veuillen, J.-Y.; Berger, C.; Conrad, E. H.; Magaud, L. Electronic Structure of Epitaxial Graphene Layers on SiC: Effect of the Substrate. *Phys. Rev. Lett.* **2007**, *99* (12), 126805.
(18) Starke, U.; Riedl, C. Epitaxial Graphene on SiC(0001) and SiC(000−1): From Surface Reconstructions to Carbon Electronics. *J. Phys.: Condens. Matter* **2009**, *21* (13), 134016.
(19) Hass, J.; Millán-Otoya, J. E.; First, P. N.; Conrad, E. H. Interface Structure of Epitaxial Graphene Grown on 4H-SiC(0001). *Phys. Rev. B: Condens. Matter Mater. Phys.* **2008**, *78* (20), 205424.
(20) Park, J. H.; Mitchel, W. C.; Smith, H. E.; Grazulis, L.; Eyink, K. G. Studies of Interfacial Layers between 4H-SiC (0001) and Graphene. *Carbon* **2010**, *48* (5), 1670−1673.
(21) Emtsev, K. V.; Speck, F.; Seyller, T.; Ley, L.; Riley, J. D. Interaction, Growth, and Ordering of Epitaxial Graphene on SiC{0001} Surfaces: A Comparative Photoelectron Spectroscopy Study. *Phys. Rev. B: Condens. Matter Mater. Phys.* **2008**, *77* (15), 155303.
(22) Kim, J.; Park, H.; Hannon, J. B.; Bedell, S. W.; Fogel, K.; Sadana, D. K.; Dimitrakopoulos, C. Layer-Resolved Graphene Transfer via Engineered Strain Layers. *Science (Washington, DC, U. S.)* **2013**, *342* (6160), 833−836.
(23) Kim, Y.; Cruz, S. S.; Lee, K.; Alawode, B. O.; Choi, C.; Song, Y.; Johnson, J. M.; Heidelberger, C.; Kong, W.; Choi, S.; Qiao, K.; Almansouri, I.; Fitzgerald, E. A.; Kong, J.; Kolpak, A. M.; Hwang, J.; Kim, J. Remote Epitaxy through Graphene Enables Two-Dimensional Material-Based Layer Transfer. *Nature* **2017**, *544* (7650), 340−343.
(24) Kong, W.; Li, H.; Qiao, K.; Kim, Y.; Lee, K.; Nie, Y.; Lee, D.; Osadchy, T.; Molnar, R. J.; Gaskill, D. K.; Myers-Ward, R. L.; Daniels, K. M.; Zhang, Y.; Sundram, S.; Yu, Y.; Bae, S.; Rajan, S.; Shao-Horn, Y.; Cho, K.; Ougazzaden, A.; Grossman, J. C.; Kim, J. Polarity Governs Atomic Interaction through Two-Dimensional Materials. *Nat. Mater.* **2018**, *17* (11), 999−1004.
(25) Jia, Y.; Ning, J.; Zhang, J.; Yan, C.; Wang, B.; Zhang, Y.; Zhu, J.; Shen, X.; Dong, J.; Wang, D.; Hao, Y. Transferable GaN Enabled by Selective Nucleation of AlN on Graphene for High-Brightness Violet Light-Emitting Diodes. *Adv. Opt. Mater.* **2020**, *8* (2), 1901632.
(26) Chang, H.; Chen, Z.; Li, W.; Yan, J.; Hou, R.; Yang, S.; Liu, Z.; Yuan, G.; Wang, J.; Li, J.; Gao, P.; Wei, T. Graphene-Assisted Quasi-van Der Waals Epitaxy of AlN Film for Ultraviolet Light Emitting Diodes on Nano-Patterned Sapphire Substrate. *Appl. Phys. Lett.* **2019**, *114* (9), 091107.
(27) Chen, Y.; Zang, H.; Jiang, K.; Ben, J.; Zhang, S.; Shi, Z.; Jia, Y.; Lü, W.; Sun, X.; Li, D. Improved Nucleation of AlN on in Situ Nitrogen Doped Graphene for GaN Quasi-van Der Waals Epitaxy. *Appl. Phys. Lett.* **2020**, *117* (5), 051601.
(28) Kim, J.; Bayram, C.; Park, H.; Cheng, C.-W.; Dimitrakopoulos, C.; Ott, J. A.; Reuter, K. B.; Bedell, S. W.; Sadana, D. K. Principle of Direct van Der Waals Epitaxy of Single-Crystalline Films on Epitaxial Graphene. *Nat. Commun.* **2014**, *5* (1), 4836.
(29) Moram, M. A.; Vickers, M. E. X-Ray Diffraction of III-Nitrides. *Rep. Prog. Phys.* **2009**, *72* (3), 036502.
(30) Etzkorn, E. V.; Clarke, D. R. Cracking of GaN Films. *J. Appl. Phys.* **2001**, *89* (2), 1025−1034.

https://doi.org/10.1021/acs.nanolett.1c00673
Nano Lett. 2021, 21, 4013−4020